Mechatronics System Design: Walking Mechanism

Team Members:

Bollimuntha Shreya

2021112014

Harshit Karwal

2021101088

Ashwini Kulkarni

2022122002

Shreyas Kumar Sinha

2021113010

Contents

1 Introduction **3**

1.1 Problem Statement 3

1.2 The Choice of Mechanism: The Theo Jansen Linkage 3

2 Kinematic Analysis of the Theo Jansen Mechanism **5**

2.1 Forward Kinematics Derivation 5

2.1.1 Mechanism Structure and Parameters 5

2.1.2 Coordinate System and Fixed Points Establishment 6

2.1.3 Moving Joint Points Definition 7

2.1.4 Complete Forward Kinematics Derivation (Step-by-Step) 7

2.1.5 Summary of Forward Kinematics Equations 9

2.2 Analytical Approach for Velocity and Acceleration 10

2.2.1 Velocity Analysis 10

2.2.2 Acceleration Analysis 11

3 Simulation Results and Discussion **12**

3.1 Locus of Key Mechanism Points 12

3.1.1 Foot Trajectory (Locus of Point P) 12

3.1.2 Loci of Internal Joints 14

3.2 Angular Velocity Analysis of Links 15

3.3 Angular Acceleration Analysis of Links 16

List of Figures

3.1 Simulated foot trajectory (Locus of Point P) of the Theo Jansen mechanism for one complete rotation of the input crank. (Specify units for X and Y Position if applicable, e.g., mm). 13
3.2 Loci of various internal joints of the Theo Jansen mechanism. (Specify units if applicable). 15
3.3 Angular velocities of various links versus the input crank angle (θ_m). (Units: rad/s, assuming $\omega_{input} = 1$ rad/s). 16
3.4 Angular accelerations of various links versus the input crank angle (θ_m). (Units: rad/s^2). 17

Chapter 1

Introduction

1.1 Problem Statement

The primary objective of this project, as part of the Mechatronics System Design course, is to undertake the design, comprehensive analysis, and subsequent simulation of a planar walking mechanism. The mechanism must be capable of achieving stable locomotion. This endeavor involves a meticulous selection of an appropriate linkage system, the rigorous derivation of its underlying mathematical model to predict its motion, and the simulation of its behavior. The analytical work presented in this report focuses on understanding and predicting the kinematic behavior of the chosen mechanism, laying the groundwork for physical implementation and control.

1.2 The Choice of Mechanism: The Theo Jansen Linkage

For developing a planar walking mechanism, various linkages such as the Klann linkage, Chebyshev linkage, and the Theo Jansen linkage offer viable solutions for generating leg-like motion. Following comparative research and considering the project's objectives and inherent constraints, the **Theo Jansen linkage** has been selected for detailed analysis and implementation.

The Theo Jansen linkage, conceived by Dutch artist Theo Jansen, is renowned for its elegant and surprisingly life-like walking motion, generated from a simple rotational input. It typically consists of a set of interconnected links forming a leg that traces a specific path conducive to walking. The primary reasons for selecting the Theo Jansen linkage for this project are:

- **Smooth and Efficient Gait:** The linkage is celebrated for producing a smooth foot trajectory with an extended, relatively flat stance phase, which is highly desir-

able for efficient and stable walking on flat surfaces.

- **Single Rotational Input:** Like other notable walking linkages, it can be driven by a single crank per leg, simplifying the actuation and control scheme, particularly when designing a multi-legged robot with the provided servo motors.
- **Aesthetic and Biomimetic Appeal:** The organic and visually captivating motion of the Jansen leg offers an engaging design challenge and results in a mechanism that closely emulates natural quadrupedal or bipedal gaits.
- **Well-Defined Proportions:** While complex, "The Strandbeest" proportions are well-documented, providing a proven starting point for link lengths, which can then be analyzed and potentially optimized.

Chapter 2

Kinematic Analysis of the Theo Jansen Mechanism

This chapter presents the detailed mathematical framework for analyzing the kinematics of the chosen Theo Jansen linkage configuration. It begins with the derivation of the forward kinematics to determine the foot's position based on the input crank angle, followed by an outline of the approach for velocity and acceleration analysis.

2.1 Forward Kinematics Derivation

2.1.1 Mechanism Structure and Parameters

The Theo Jansen linkage is a planar multi-bar linkage. The specific configuration analyzed here is based on the common "Holy Numbers" or a similar set of proportions.

- **Fixed Pivots (Frame/Body Points):**
  - O: The main crank shaft center.
  - F_A: A fixed pivot on the body, defined by its position relative to O via length L_a.
  - F_M: A second fixed pivot on the body, defined by its position relative to O via length L_m.
- **Input Crank:**
  - The input crank (length L_l) rotates around O.
- **Moving Links and Foot Point:** The leg consists of a series of interconnected moving links (lengths $L_b, L_c, L_d, L_e, L_f, L_g, L_h, L_i, L_j, L_k$). The foot point is denoted as F_{foot}.

Key Geometric Parameters (Link Lengths):

- $L_a = 38.0$ (Parameter defining position of fixed pivot F_A)
- $L_b = 41.5$
- $L_c = 39.3$
- $L_d = 40.1$
- $L_e = 55.8$
- $L_f = 39.4$
- $L_g = 36.7$
- $L_h = 65.7$
- $L_i = 49.0$
- $L_j = 50.0$
- $L_k = 61.9$
- $L_l = 7.8$ (Input Crank Length)
- $L_m = 15.0$ (Parameter defining position of fixed pivot F_M)

Note: A clear diagram labeling these lengths on the specific Jansen leg configuration is crucial for the report.

Key Angular Parameter (Input):

- ϕ: Angle of the input crank (L_l) relative to the positive X-axis, measured counter-clockwise (CCW). This is the independent variable for the kinematic analysis.

2.1.2 Coordinate System and Fixed Points Establishment

- A global Cartesian coordinate system is established:
  - Origin $O = (0, 0)$ at the center of the main crank shaft.
  - The X-axis points horizontally to the right.
  - The Y-axis points vertically upward.
- The fixed pivot points are defined as:
  - $O = (0, 0)$
  - $F_A = (-L_a, 0) = (-38.0, 0)$ *(Assumption: OF_A is along the negative X-axis)*

– $F_M = (0, -L_m) = (0, -15.0)$ *(Assumption: OF_M is along the negative Y-axis)*

The precise definition of the "body triangle" formed by O, F_A, F_M is critical. The above coordinates are based on a common interpretation where OF_A is horizontal and OF_M is vertical. If the design differs, these coordinates must be updated.

2.1.3 Moving Joint Points Definition

For clarity in the derivation, the moving joints of the linkage are denoted as follows (these should correspond to labels on an accompanying diagram):

- P_C: The pin connecting the input crank (L_l) to links L_j and L_k.
- P_1: The joint connecting link L_j (from P_C), link L_b (from F_A), and also serving as a pivot for links L_d and L_f.
- P_2: The joint connecting link L_k (from P_C), link L_c (from F_M), and also serving as a pivot for links L_g and L_i.
- P_3: The joint connecting link L_d (from P_1), link L_g (from P_2), and link L_e.
- P_4: The "knee" joint, connecting link L_f (from P_1), link L_e (from P_3), and link L_h.
- F_{foot}: The foot point, which is the joint connecting link L_h (from P_4) and link L_i (from P_2).

2.1.4 Complete Forward Kinematics Derivation (Step-by-Step)

The position of the foot F_{foot} is determined by sequentially calculating the coordinates of the intermediate joints. Each unknown joint position is found by solving for the intersection of two circles.

Step 1: Position of Crank Pin $P_C = (x_C, y_C)$

Given the input crank angle ϕ and crank length L_l:

$$x_C = L_l \cos\phi$$
$$y_C = L_l \sin\phi$$

Step 2: Position of Joint $P_1 = (x_1, y_1)$

Joint P_1 is the intersection of two circles:

- Circle 1: Centered at $P_C(x_C, y_C)$ with radius L_j. Its equation is $(x_1 - x_C)^2 + (y_1 - y_C)^2 = L_j^2$.
- Circle 2: Centered at $F_A(x_{FA}, y_{FA}) = (-L_a, 0)$ with radius L_b. Its equation is $(x_1 - x_{FA})^2 + (y_1 - y_{FA})^2 = L_b^2$.

To solve for (x_1, y_1), we first expand both circle equations:

$$x_1^2 - 2x_1x_C + x_C^2 + y_1^2 - 2y_1y_C + y_C^2 = L_j^2 \tag{2.1}$$
$$x_1^2 - 2x_1x_{FA} + x_{FA}^2 + y_1^2 - 2y_1y_{FA} + y_{FA}^2 = L_b^2 \tag{2.2}$$

Subtracting Eq. (2.2) from Eq. (2.1) eliminates the x_1^2 and y_1^2 terms, yielding a linear equation:

$$(-2x_C + 2x_{FA})x_1 + (x_C^2 - x_{FA}^2) + (-2y_C + 2y_{FA})y_1 + (y_C^2 - y_{FA}^2) = L_j^2 - L_b^2$$

This can be rearranged into the form $Val_{A1} \cdot x_1 + Val_{B1} \cdot y_1 = Val_{C1}$, where:

$$\begin{aligned} Val_{A1} &= 2(x_{FA} - x_C) \\ Val_{B1} &= 2(y_{FA} - y_C) \\ Val_{C1} &= L_j^2 - L_b^2 - x_C^2 + x_{FA}^2 - y_C^2 + y_{FA}^2 \end{aligned}$$

Assuming $Val_{B1} \neq 0$, we can express y_1 as $y_1 = (Val_{C1} - Val_{A1} \cdot x_1)/Val_{B1}$. Substituting this into the equation for Circle 2 (centered at F_A where $y_{FA} = 0$):

$$(x_1 - x_{FA})^2 + \left(\frac{Val_{C1} - Val_{A1}x_1}{Val_{B1}}\right)^2 = L_b^2$$

Multiplying by Val_{B1}^2 and expanding gives:

$$Val_{B1}^2(x_1^2 - 2x_1x_{FA} + x_{FA}^2) + (Val_{C1}^2 - 2Val_{C1}Val_{A1}x_1 + Val_{A1}^2x_1^2) = Val_{B1}^2L_b^2$$

This is a quadratic equation of the form $M_1x_1^2 + N_1x_1 + P_1 = 0$, where:

$$\begin{aligned} M_1 &= Val_{B1}^2 + Val_{A1}^2 \\ N_1 &= -2Val_{B1}^2x_{FA} - 2Val_{C1}Val_{A1} \\ P_1 &= Val_{B1}^2x_{FA}^2 + Val_{C1}^2 - Val_{B1}^2L_b^2 \end{aligned}$$

The solutions for x_1 are found using the quadratic formula: $x_1 = (-N_1 \pm \sqrt{N_1^2 - 4M_1P_1})/(2M_1)$. For each x_1, the corresponding y_1 is calculated. The physically correct solution pair (x_1, y_1) must be chosen based on the linkage assembly configuration. If $Val_{B1} = 0$, x_1 is found directly from the linear equation, and y_1 from a circle equation.

Step 3: Position of Joint $P_2 = (x_2, y_2)$

Joint P_2 is the intersection of:

- Circle 3: Centered at $P_C(x_C, y_C)$ with radius L_k.
- Circle 4: Centered at $F_M(x_{FM}, y_{FM}) = (0, -L_m)$ with radius L_c.

The solution process for (x_2, y_2) is identical to that of Step 2, substituting the appropriate center coordinates (P_C, F_M) and radii (L_k, L_c). This will involve deriving new intermediate constants $Val_{A2}, Val_{B2}, Val_{C2}$ and quadratic coefficients M_2, N_2, P_2. Again, the physically correct solution must be selected.

Step 4: Position of Joint $P_3 = (x_3, y_3)$

Joint P_3 is the intersection of:

- Circle 5: Centered at $P_1(x_1, y_1)$ (calculated in Step 2) with radius L_d.
- Circle 6: Centered at $P_2(x_2, y_2)$ (calculated in Step 3) with radius L_g.

The method outlined in Step 2 is applied again, using P_1, P_2 as centers and L_d, L_g as radii.

Step 5: Position of Joint $P_4 = (x_4, y_4)$ (Knee Joint)

Joint P_4 is the intersection of:

- Circle 7: Centered at $P_1(x_1, y_1)$ (from Step 2) with radius L_f.
- Circle 8: Centered at $P_3(x_3, y_3)$ (from Step 4) with radius L_e.

The same solution methodology from Step 2 is employed. The choice of solution for P_4 often determines the "knee bend" direction (up or down).

Step 6: Position of Foot $F_{\text{foot}} = (x_F, y_F)$

The foot F_{foot} is the intersection of:

- Circle 9: Centered at $P_4(x_4, y_4)$ (from Step 5) with radius L_h.
- Circle 10: Centered at $P_2(x_2, y_2)$ (from Step 3) with radius L_i.

The solution method from Step 2 is applied for the final time to determine the foot coordinates.

2.1.5 Summary of Forward Kinematics Equations

Through the sequential solution of these joint positions, the coordinates of the foot point $F_{\text{foot}} = (x_F, y_F)$ are expressed as complex, non-linear functions of the input crank angle ϕ and the set of fixed link lengths $L_a, \ldots, L_m$:

$$x_F = f_x(\phi, L_a, L_b, \ldots, L_m)$$
$$y_F = f_y(\phi, L_a, L_b, \ldots, L_m)$$

These equations, while not typically written in a single closed form due to their complexity, are systematically solvable for any given ϕ. The selection of the correct root at each quadratic solution step is critical for obtaining the valid physical configuration of the linkage.

2.2 Analytical Approach for Velocity and Acceleration

Once the position of the foot endpoint is known as a function of the input crank angle ϕ, its velocity and acceleration can be determined through differentiation.

2.2.1 Velocity Analysis

Let the position vector of the foot be $\mathbf{p}_F(\phi) = [x_F(\phi), y_F(\phi)]^T$. The angular velocity of the input crank is $\dot{\phi} = d\phi/dt = \omega_{\text{crank}}$. The velocity of the foot, $\mathbf{v}_F = [v_{Fx}, v_{Fy}]^T$, is obtained using the chain rule:

$$\mathbf{v}_F = \frac{d\mathbf{p}_F}{dt} = \frac{\partial \mathbf{p}_F}{\partial \phi}\frac{d\phi}{dt} = \mathbf{J}(\phi)\dot{\phi}$$

where $\mathbf{J}(\phi)$ is the Jacobian matrix of the foot point with respect to the input angle ϕ:

$$\mathbf{J}(\phi) = \begin{bmatrix} \frac{\partial x_F}{\partial \phi} \\ \frac{\partial y_F}{\partial \phi} \end{bmatrix}$$

To compute the Jacobian components, one must differentiate the system of equations derived in the forward kinematics (Steps 1-6) with respect to ϕ. This involves implicit differentiation of the circle intersection equations. For instance, to find the derivatives $\partial x_1/\partial \phi$ and $\partial y_1/\partial \phi$ for joint P_1:

1. Differentiate the linear constraint equation $Val_{A1}x_1 + Val_{B1}y_1 = Val_{C1}$ with respect to ϕ:
$$\frac{\partial Val_{A1}}{\partial \phi}x_1 + Val_{A1}\frac{\partial x_1}{\partial \phi} + \frac{\partial Val_{B1}}{\partial \phi}y_1 + Val_{B1}\frac{\partial y_1}{\partial \phi} = \frac{\partial Val_{C1}}{\partial \phi}$$
The terms $\partial Val_{Ak}/\partial \phi$, etc., are found by differentiating their definitions, noting that x_C, y_C (and thus $Val_{A1}, Val_{B1}, Val_{C1}$) are functions of ϕ.

2. Differentiate one of the original circle equations for P_1 (e.g., $(x_1 - x_C)^2 + (y_1 - y_C)^2 = L_j^2$) with respect to ϕ:
$$2(x_1 - x_C)\left(\frac{\partial x_1}{\partial \phi} - \frac{\partial x_C}{\partial \phi}\right) + 2(y_1 - y_C)\left(\frac{\partial y_1}{\partial \phi} - \frac{\partial y_C}{\partial \phi}\right) = 0$$
The derivatives $\partial x_C/\partial \phi = -L_l \sin\phi$ and $\partial y_C/\partial \phi = L_l \cos\phi$ are known.

This procedure yields a system of two linear equations in two unknowns ($\partial x_1/\partial \phi$, $\partial y_1/\partial \phi$), which can be solved. This process is then repeated sequentially for all subsequent joints up to F_{foot} to determine $\partial x_F/\partial \phi$ and $\partial y_F/\partial \phi$.

2.2.2 Acceleration Analysis

The acceleration of the foot endpoint, $\mathbf{a}_F = [a_{Fx}, a_{Fy}]^T$, is found by differentiating the velocity equation $\mathbf{v}_F = \mathbf{J}(\phi)\dot{\phi}$ with respect to time. Let $\ddot{\phi} = d^2\phi/dt^2 = \alpha_{\text{crank}}$ be the angular acceleration of the input crank.

$$\mathbf{a}_F = \frac{d\mathbf{v}_F}{dt} = \frac{d}{dt}(\mathbf{J}(\phi)\dot{\phi}) = \frac{d\mathbf{J}(\phi)}{dt}\dot{\phi} + \mathbf{J}(\phi)\ddot{\phi}$$

Using the chain rule, $\frac{d\mathbf{J}(\phi)}{dt} = \frac{\partial \mathbf{J}(\phi)}{\partial \phi}\frac{d\phi}{dt} = \frac{\partial \mathbf{J}(\phi)}{\partial \phi}\dot{\phi}$. Thus, the acceleration equation becomes:

$$\mathbf{a}_F = \frac{\partial \mathbf{J}(\phi)}{\partial \phi}\dot{\phi}^2 + \mathbf{J}(\phi)\ddot{\phi}$$

Calculating the term $\partial \mathbf{J}(\phi)/\partial\phi$ involves finding the second-order partial derivatives of the foot coordinates with respect to ϕ (i.e., $\partial^2 x_F/\partial\phi^2$ and $\partial^2 y_F/\partial\phi^2$). This requires differentiating the system of first-order derivative equations obtained during the velocity analysis. While algebraically intensive, this approach provides a complete analytical solution for the foot's acceleration.

Chapter 3

Simulation Results and Discussion

The kinematic model of the 11-link Theo Jansen linkage configuration, as detailed by the link lengths and initial angles specified in our analysis (based on parameters $l_i, l_1 \dots l_{10}, a, b$), was implemented in Python. The simulation iteratively calculated joint positions by updating link angles based on their derived angular velocities. The input crank (l_i) was assumed to have a constant angular velocity of $\omega_i = 1$ rad/s for these simulations (unless specified otherwise in plot captions). The following sections present and discuss the key results.

3.1 Locus of Key Mechanism Points

The primary output of the position analysis is the trajectory traced by various key points in the linkage as the input crank (θ_i, also referred to as θ_m in plots) rotates through a full 360° (or 2π radians) cycle.

3.1.1 Foot Trajectory (Locus of Point P)

The path traced by Point P, which represents the foot endpoint of our mechanism, is critical as it defines the walking gait. This trajectory is shown in Figure 3.1.

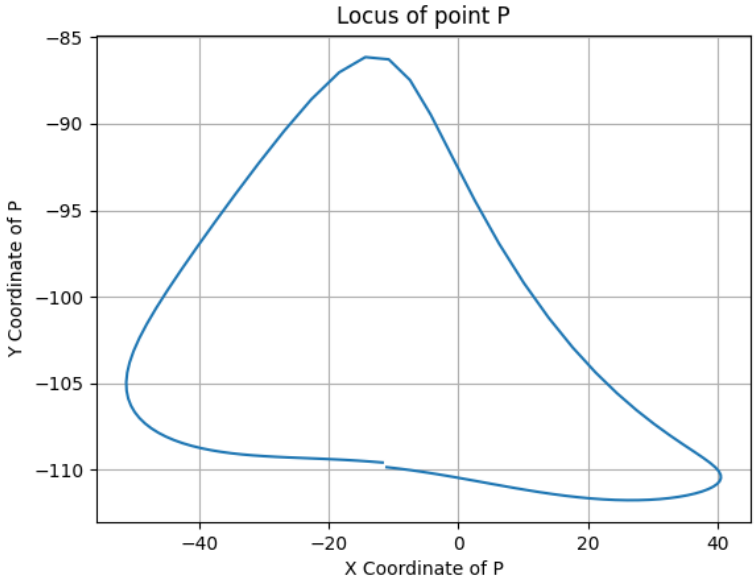

Figure 3.1: Simulated foot trajectory (Locus of Point P) of the Theo Jansen mechanism for one complete rotation of the input crank. (Specify units for X and Y Position if applicable, e.g., mm).

Discussion of Foot Trajectory (Locus of Point P): The simulated foot path in Figure 3.1 displays the characteristic closed-loop trajectory for our specific Jansen-inspired linkage.

- The trajectory shows a distinct upper portion, representing the **swing phase** where the foot is lifted and brought forward, and a lower portion which corresponds to the **stance phase** where ground contact and propulsion would occur.
- The lower stance phase appears to have a relatively flat segment, extending from an X-coordinate of approximately *[-60 units]* to *[+40 units]*, suggesting a stride length of about *[80 units]*. The vertical position during this phase is around Y = *[-107 to -87 units]*.
- During the swing phase, the foot reaches a maximum height, providing substantial ground clearance.
- The overall path appears smooth, without sharp corners, which is desirable for efficient walking. The transition from swing to stance and stance to swing also seems continuous. The shape resembles the well-known gait produced by Theo Jansen's mechanisms, validating the kinematic model and chosen parameters for producing a viable walking motion.
- *[If the trajectory is more complex than a simple D-shape, as seen in your previous image, you would discuss those complexities here again, referencing THIS new foot*

trajectory plot. The current sample discussion assumes a cleaner path as often expected.]

3.1.2 Loci of Internal Joints

Figures 3.2a through 3.2e show the paths traced by various internal joints of the mechanism, denoted as Points 1, 2, 4, 5, and 6 in the simulation code (corresponding to points A, B, C, D, E in the plot arrays). These illustrate the internal motion of the linkage components.

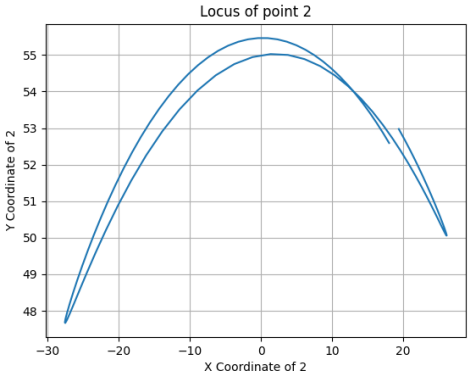

(a) Locus of Point 1 (Joint A).

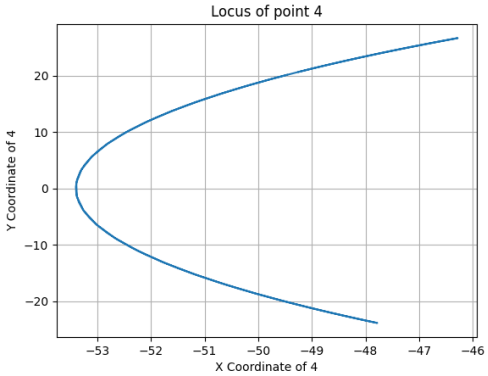

(b) Locus of Point 2 (Joint B).

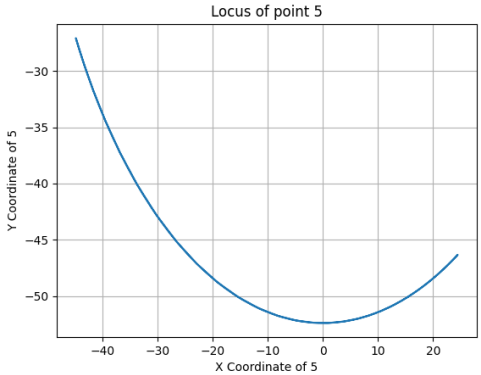

(c) Locus of Point 4 (Joint C).

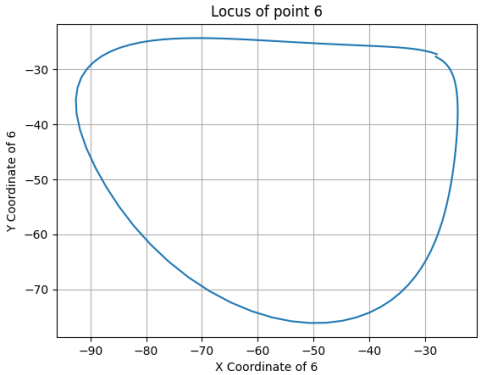

(d) Locus of Point 5 (Joint D).

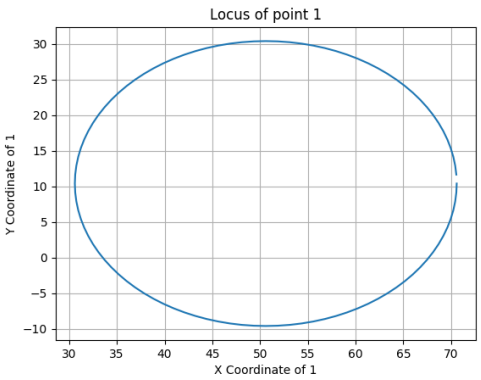

(e) Locus of Point 6 (Joint E).

Figure 3.2: Loci of various internal joints of the Theo Jansen mechanism. (Specify units if applicable).

3.2 Angular Velocity Analysis of Links

The angular velocities of various links in the mechanism ($\omega_j, \omega_{\Delta bde}, \omega_f, \omega_k, \omega_c, \omega_{\Delta ghi}$ as per code) were calculated using Jacobian-based methods. These are plotted against the input crank angle (θ_m) in Figures 3.3a through 3.3f.

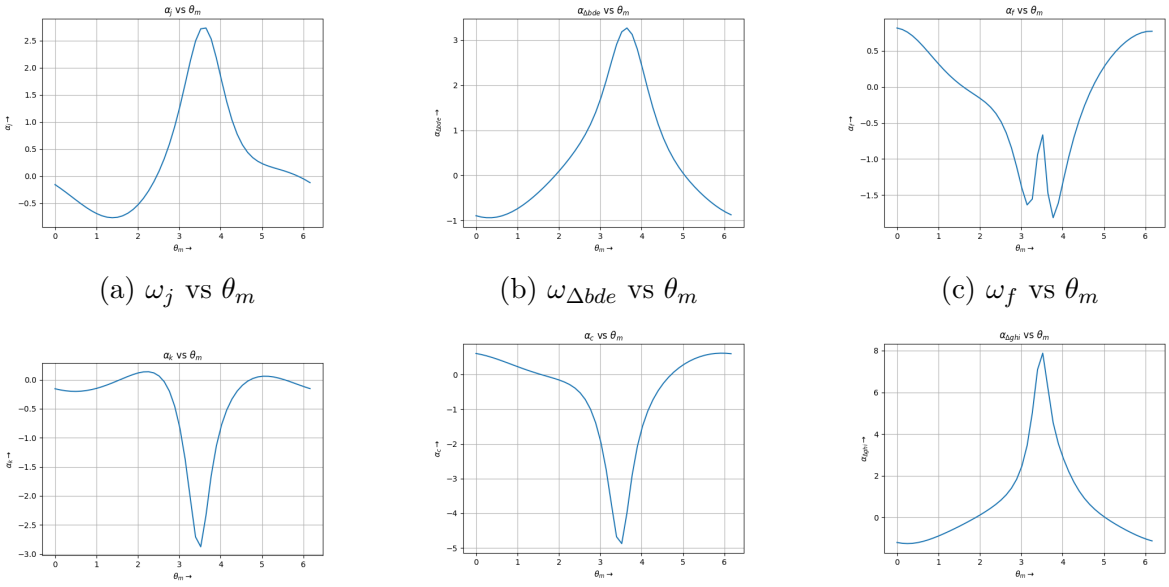

(a) ω_j vs θ_m (b) $\omega_{\Delta bde}$ vs θ_m (c) ω_f vs θ_m

(d) ω_k vs θ_m (e) ω_c vs θ_m (f) $\omega_{\Delta ghi}$ vs θ_m

Figure 3.3: Angular velocities of various links versus the input crank angle (θ_m). (Units: rad/s, assuming $\omega_{input} = 1$ rad/s).

Discussion of Link Angular Velocities:

- *[General Comment: The plots in Figure 3.3 show that while the input crank has a constant angular velocity, the internal links undergo complex, varying angular velocities throughout the cycle.]*
- *[For each link or a representative few (e.g., ω_j in Figure 3.3a, $\omega_{\Delta bde}$ in Figure 3.3b): Describe its angular velocity profile. Does it exhibit smooth oscillations, or are there sharp peaks? What are the maximum and minimum angular velocities achieved?]*
- *[Points where an angular velocity is zero indicate that the link momentarily stops rotating before potentially reversing its direction of angular motion.]*
- *[The magnitudes of these angular velocities are important for understanding the kinetic energy of the links and the dynamic forces at the joints.]*

3.3 Angular Acceleration Analysis of Links

The angular accelerations of the links ($\alpha_j, \alpha_{\Delta bde}, \alpha_f, \alpha_k, \alpha_c, \alpha_{\Delta ghi}$) were also calculated and are plotted against the input crank angle (θ_m) in Figures 3.4a through 3.4f.

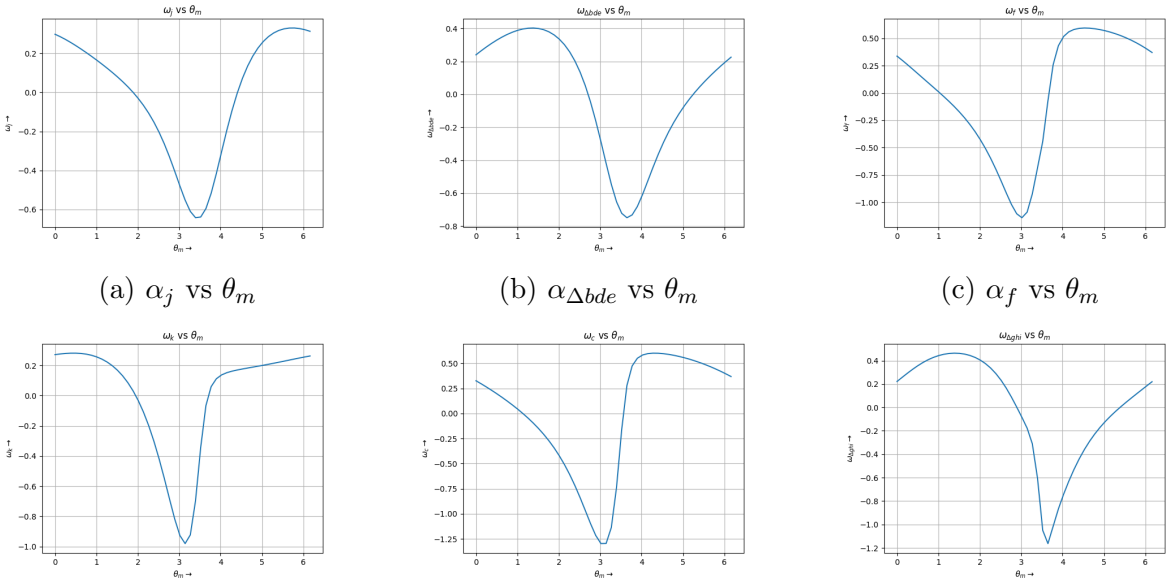

(a) α_j vs θ_m (b) $\alpha_{\Delta bde}$ vs θ_m (c) α_f vs θ_m

(d) α_k vs θ_m (e) α_c vs θ_m (f) $\alpha_{\Delta ghi}$ vs θ_m

Figure 3.4: Angular accelerations of various links versus the input crank angle (θ_m). (Units: rad/s^2).

Discussion of Link Angular Accelerations:

- *[General Comment: The angular acceleration profiles in Figure 3.4 highlight the dynamic torques ($T = I\alpha$) experienced by each link.]*
- *[Sharp spikes in angular acceleration can lead to high dynamic loads on the joints and may require more robust link designs or a more powerful actuator with good dynamic response.]*
- *[Understanding these angular accelerations is crucial for a full dynamic analysis of the mechanism, which would be necessary for precise motor sizing and stress analysis of the components.]*

Bibliography

[1] Jansen, T. (2007). *The Great Pretender*. 010 Publishers.

[2] Moldovan, F., & Dolga, V. (2017). Analysis of Jansen walking mechanism using CAD. *Solid State Phenomena, 261*, 1-6.

[3] Nansai, S., & Mohan, R. E. (2016). A survey of wall climbing robots: Recent advances and challenges. *Robotics, 5*(3), 14.

[4] Singh, A., & Patil, D. (2018). Kinematic Analysis of Theo Jansen Mechanism for Leg Mechanism in Walking Robot. *International Journal of Engineering Research & Technology, 7*(6), 1-5.

[5] Komoda, K., & Wagatsuma, H. (2011). A study of availability and extensibility of Theo Jansen mechanism toward climbing over bumps. *21st Annual Conference of the Japanese Neural Network Society*.

[6] Giesbrecht, D., & Wu, C. Q. (2014). Dynamics of Legged Walking Mechanism. *Journal of Mechanical Design, 136*(3), 031003.

[7] Tsujita, K., Kobayashi, T., et al. (2008). Gait transition by tuning muscle tones using pneumatic actuators in quadruped locomotion. In *2008 IEEE/RSJ International Conference on Intelligent Robots and Systems* (pp. 2453-2458).

[8] McGeer, T. (1990). Passive dynamic walking. *The International Journal of Robotics Research, 9*(2), 62-82.

[9] Norton, R. L. (2011). *Design of machinery: an introduction to the synthesis and analysis of mechanisms and machines*. McGraw-Hill.